The Use of Voltage Transformers for the Measurement of Power System Subharmonics in Compliance With International Standards

Gabriella Crotti, Giovanni D'Avanzo, Palma Sara Letizia, and Mario Luiso, *Member, IEEE*

***Abstract*— The measurement of subharmonics in distribution systems requires instrument transformers to reduce voltage and current to levels fitting with the low-voltage input of the power quality (PQ) instruments. The in-force international standards establish algorithms and methods for detecting, measuring, and reporting subharmonics. In particular, the IEC 61000-4-7 suggests performing the discrete Fourier transform over basic time frames of ten cycles (12 cycles) for the 50-Hz (60 Hz) power frequency. Considering the case of 50-Hz constant power frequency, the spectral analysis is performed with a fixed spectral resolution of 5 Hz; thus, subharmonics with a frequency not integer multiple of 5 Hz could introduce inaccuracies in the measurements because of the spectral leakage. In this framework, this article investigates the additional error contributions that can be introduced by voltage transformers (VTs) used, at the input of PQ instruments, to measure subharmonics in compliance with international standards. The analysis is conducted through numerical simulations and experimental tests on two commercial VTs based on different operating principles. Results show that the use of a VT to measure subharmonics, in compliance with international standards, could introduce higher additional errors compared to the ratio errors of the same device evaluated at subharmonic frequencies.**

***Index Terms*— Harmonics, inductive voltage transformers (VTs), instrument transformer (IT), low-power VTs (LPVTs), power quality (PQ), power system measurements, subharmonics.**

I. Introduction

THE large-scale introduction of distributed generation systems based on renewable sources and the spreading of electronic loads is turning the power grids into increasingly complex systems characterized by increasing disturbances. In this scenario, the accurate monitoring of power quality (PQ) parameters is gaining more and more importance [1], [2], [3], and several international standards [4], [5], [6], [7], [8], [9] dealing with this topic have been released.

The measurement chain for PQ monitoring in medium-voltage (MV) and high-voltage (HV) systems commonly includes instrument transformers (ITs) to scale the voltage and current to levels fitting with the input of PQ instruments (PQIs). Nevertheless, the performance of ITs in the presence of PQ phenomena represents an issue only partially addressed in the literature [10], [11], [12], [13] and technical reports [14].

Among the PQ phenomena, the monitoring of harmonics and interharmonics plays a crucial role because their presence causes many problems, such as overheating of conductors, losses in power transformers, improper functioning of electric motors, and damage to power factor capacitors.

Subharmonics are particular cases of interharmonics; in fact, they are defined as components with frequencies lower and, consequently, not integer multiples of the fundamental frequency at which the supply system is designed to operate. Subharmonics are injected into the power grid by distributed generation systems, such as wind farms [15], [16], hydropowers [17] or photovoltaic plants [18], and loads, such as arc furnaces and cycloconverters [19], [20], [21].

The detection and measurement of power system subharmonics are covered by international standards [22], [23], which define the measurement methods, time frames, and indices. For the evaluation of subharmonics, as well as harmonics and interharmonics, the discrete Fourier transform (DFT) performed with a rectangular window is one of the processing tools recommended by the standard [22], which indicates as basic measurement time frame an interval equal to ten cycles (12 cycles) for 50-Hz (60-Hz) systems. Considering power systems operating at 50 Hz, frequency variations over time can occur, leading to variable time frames that are not always equal to 200 ms. In the following, this article will refer to the specific case in which the power frequency is constant and fixed to 50 Hz. This restriction is intended to simplify the analysis by avoiding the error contribution due to the algorithm for power frequency estimation. However, the presented results hold true regardless of the specific case that is taken into account, as long as the additional error of the power frequency synchronization algorithm with the network frequency is considered.

Manuscript received 7 June 2022; revised 24 August 2022; accepted 27 August 2022. Date of publication 5 September 2022; date of current version 27 September 2022. The work here presented has received funding from EMPIR (European Metrology Programme for Innovation and Research) 19NRM05 IT4PQ. This project 19NRM05 IT4PQ has received funding from the EMPIR programme co-financed by the Participating States and from the European Union's Horizon 2020 research and innovation programme. The Associate Editor coordinating the review process was Dr. Paolo Attilio Pegoraro. *(Corresponding author: Mario Luiso.)*

Gabriella Crotti and Palma Sara Letizia are with the Divisione Metrologia dei materiali innovativi e scienze della vita, Istituto Nazionale di Ricerca Metrologica, 10135 Turin, Italy (e-mail: g.crotti@inrim.it; p.letizia@inrim.it).

Giovanni D'Avanzo is with the Dipartimento Tecnologie di trasmissione e distribuzione (TTD), Ricerca sul Sistema Energetico S.p.A., 20134 Milan, Italy, and also with the Dipartimento di Ingegneria, Università degli Studi della Campania "Luigi Vanvitelli," 81031 Aversa, Italy (e-mail: giovanni.davanzo@rse-web.it).

Mario Luiso is with the Dipartimento di Ingegneria, Università degli Studi della Campania "Luigi Vanvitelli," 81031 Aversa, Italy (e-mail: mario.luiso@unicampania.it).

Digital Object Identifier 10.1109/TIM.2022.3204318

Under the assumption of power frequency constant and equal to 50 Hz, the spectral analysis for the measurement of power system subharmonics is performed with a fixed spectral resolution equal to 5 Hz. However, the resolution of 5 Hz might not be sufficient for proper detection of subharmonics, especially when subharmonics with a frequency not integer multiple of 5 Hz are present, since they produce spectral leakage that can badly affect the results [24].

Crotti *et al.* [21] have experimentally shown how subharmonics, having realistic amplitudes and frequencies, can impact the performance of inductive voltage transformers (VTs) when they are used for harmonic measurements.

Taking another step forward in this context, this article focuses on the performances of inductive VTs and low-power VTs (LPVTs), in the measurements of subharmonics, when these measurements are performed following the guidelines given by the international standard [22]. The study is carried out in three stages. In the first stage, the case of an ideal PQI compliant with [22] is considered. Numerical simulations are used to study the errors introduced by such a PQI in the measurement of the first interharmonic group [5, 45] Hz in the presence of subharmonics that cause spectral leakage (i.e., in the ranges]0, 5[and]45, 50[Hz). Then, different numerical simulations are performed to study what happens when an IT is used upstream of a PQI for the measurement of the first interharmonic group. In particular, several ITs are simulated with the aim of performing a sensitivity analysis regarding how the IT error is affected by its different frequency response parameters. Finally, experimental tests on two commercial devices are carried out to accurately quantify their error contributions in the measurement of subharmonics in accordance with [22].

The activity presented in this article is developed in the framework of a European metrology research project: EMPIR project 19NRM05 IT4PQ [25]. The main goal of this project is to establish the methods and procedures for assessing the errors introduced by ITs when they are involved in PQ applications.

This article is organized as follows. Section II discusses the algorithms for the subharmonics measurement and introduces possible performance indices (PIs) for quantifying the errors introduced by ITs. Sections III and IV show the results of numerical simulations for the evaluation of the deviation introduced, respectively, by an ideal PQI, compliant with [22] and [23], and by a linear IT in the subharmonics measurement. Section VI describes the generation and measurement setup for the laboratory characterization of inductive VTs and LPVTs. Section VII provides experimental results related to tests performed on a commercial inductive VT and a commercial LPVT. Finally, Section VIII draws the conclusions.

II. Standard Methods and Indices for Subharmonic Measurements

This section introduces the standard methods and indices to evaluate the subharmonics, but more in general also harmonic and interharmonic components, in power systems. The standard methods and indices are mainly defined in standards dealing with harmonics and interharmonics measurement [4], [5], [6], [7], [8], [9]. It is important to highlight that this work refers to methods and indices defined for Class A PQIs (PQI-A) used when accurate measurements are necessary [5], [6], [7], [8], [9]. Without loss of generality, this article will refer to 50-Hz power systems; very similar results can be obtained for 60-Hz power systems by changing the involved frequencies and the duration of the time frame chosen for the analysis of the waveforms. Thus, with particular reference to a 50-Hz constant power system, the standard [22] suggests using the DFT on time frames of 200 ms, resulting in a fixed frequency resolution equal to 5 Hz, for the measurement of harmonic and interharmonic components.

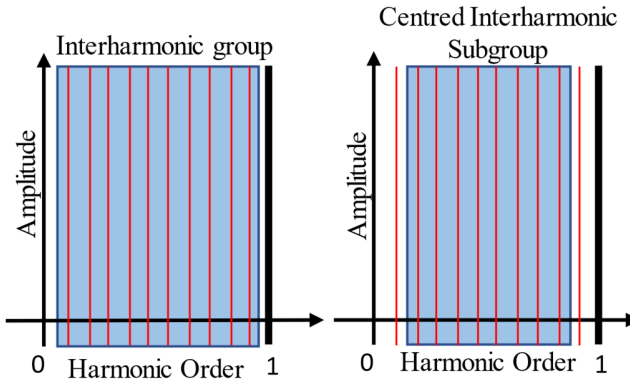

Fig. 1. Interharmonic group and centered interharmonic subgroup.

Since the frequencies of interest in this work are in the range]0, 50[Hz, the measurement indices used to quantify the interharmonic components at frequencies lower than 50 Hz are the interharmonic group Y_g and the gapless interharmonic centered subgroup Y_{csg} [22], as illustrated in Fig. 1 and defined as in (1) and (2) considering the case of $h = 0$

$$Y_g = \sqrt{\sum_{m=1}^{8} V_{h\cdot f_1+m\cdot r}^2} \tag{1}$$

$$Y_{\mathrm{csg}} = \sqrt{Y_g^2 - V_{h\cdot f_1+r}^2 - V_{h\cdot f_1+8\cdot r}^2} \tag{2}$$

where Y_g is the Root Mean Square (RMS) value of all the interharmonic components in the frequency interval between two consecutive harmonic frequencies; Y_{csg} is the RMS value of the interharmonic group excluding the interharmonic components adjacent to the harmonics; $V_{h\cdot f_1+m\cdot r}^2$ is the RMS value of the voltage at $(h\cdot f_1 + m\cdot r)$ frequency; f_1 is the power frequency; and r is the frequency resolution equal to 5 Hz.

The conventional indices used to evaluate the ITs accuracy and assign the accuracy class are the ratio and phase errors defined at power frequency [26], [27]. In this work, the definition of ratio and phase errors has been extended, considering the indices in (1) and (2). The IT-PI is defined as follows:

$$\varepsilon_\eta = \frac{k_r Y_{\eta,s} - Y_{\eta,p}}{Y_{\eta,p}} \tag{3}$$

where $k_r = V_{p,r}/V_{s,r}$ is the rated transformation ratio at 50 Hz ($V_{p,r}$ and $V_{s,r}$ are the rated primary and secondary voltages at 50 Hz); $Y_{\eta,p}$ and $Y_{\eta,s}$ are the interharmonic group ($\eta = g$)

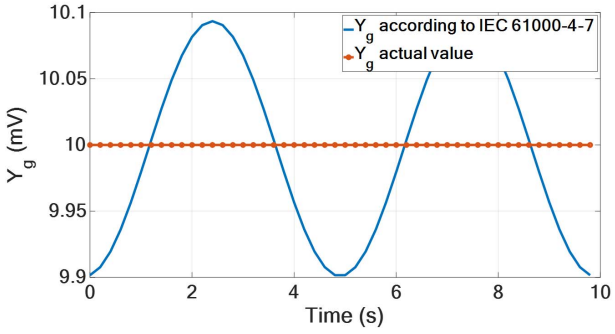

Fig. 2. Comparison between time behavior of the actual value (circle marker) of Y_g and the value evaluated according to the IEC 61000-4-7 standard (solid line) of a voltage signal including 1 V at 50 Hz and 10 mV subharmonic at 5.1 Hz.

or the gapless centered interharmonic subgroup ($\eta = csg$) at the primary and secondary sides of the IT. These indices allow evaluating the accuracy of the ITs when they are used for the measurement of subharmonics in compliance with [22].

As mentioned in Section I, the use of the DFT on a time frame of 200 ms, when the analyzed signal contains components with frequencies not integer multiple of 5 Hz, produces inaccurate results due to the spectral leakage [28], [29], [30], [31], [32]. In fact, in these cases, since the periodicity of the signal is longer than 200 ms, the portions of the signal analyzed in two adjacent 200-ms time frames differ among them. Therefore, the DFT produces different results over different time frames, causing a time-varying behavior of the analyzed quantities. An example is provided in Fig. 2 that shows two Y_g curves of the same voltage signal composed of a fundamental tone, at 50 Hz and 1 V, and by a subharmonic, at 5.1 Hz and 10 mV. The circle marker curve is the Y_g actual value, obtained performing the DFT over a time frame equal to the signal periodicity (10 s), whereas the solid line is the Y_g value obtained performing the DFT over 200 ms. As it can be observed, because of the algorithm, the measured Y_g has a mean value of 10 mV, but it oscillates in the range [9.9, 10.09] mV.

This example highlights that there can be situations in which, even if the signal is stationary, since it is analyzed over a time frame shorter than its periodicity, the indices in (1) and (2) have a time-varying behavior, leading also the PIs in (3) to have the same behavior. To take into account the variability of (3), it is convenient to introduce the index (4), which quantifies the maximum absolute value of (3)

$$\xi_\eta = \max_{\cup\tau_n} |\varepsilon_\eta| \tag{4}$$

where $\cup\tau_n$ is the union of the nonoverlapping time frames (each one ten cycles of the 50-Hz tone) in which ε_η is evaluated.

III. Impact of Signal Processing

This section aims at quantifying the error introduced by the signal processing suggested by [22] for the measurement of Y_g and Y_{csg} when subharmonics with frequencies in the range [0.1, 49.9] Hz are present in the analyzed signal.

For this purpose, two different simulations are performed. In the first step, only subharmonic components in the range [5, 45] Hz are considered, whereas, in the second step, also, the subharmonics outside this frequency range are included in the analysis. It is worth highlighting that the first step of the analysis focuses on the first interharmonic group defined by [22]. Additional tones, in the ranges]0, 5[and]45, 50[Hz, adjacent to the first interharmonic group, are included in the second step. As a result of the mismatch between the periods of these components and the time frame used for the analysis, they can introduce spectral leakage into the [5, 45] Hz frequency range.

The PIs used for this analysis are the same introduced in Section II for the IT [see (3) and (4)]. In particular, ε_η is obtained by assuming the following.

1) $k_r = 1$ V/V.
2) $Y_{\eta,p}$ equal to the actual value (obtained by performing the DFT on a time frame equal to an integer multiple of the signal periodicity).
3) $Y_{\eta,s}$ is equal to the value calculated by implementing the measurement method indicated by the standard [22].

A. Case of a Single Subharmonic

In the first case, a voltage signal composed of a fundamental tone plus one subharmonic, as described in (5), is numerically simulated

$$s_1(t) = A_f \sin(2\pi f_0 t) + A_{\text{sub-h}} \sin(2\pi f_{\text{sub-h}} t + \varphi_{\text{sub-h}}). \tag{5}$$

The fundamental tone has amplitude A_f equal to 1 V, and the frequency f_0 is fixed to 50 Hz; in this way, using a sampling frequency equal to an integer multiple of the signal frequency, there is no need for a specific technique to estimate the signal frequency. Therefore, there is perfect synchronization between the fundamental tone and the 200-ms time frame, avoiding the spectral leakage contribution due to the fundamental component. The subharmonic has amplitude $A_{\text{sub-h}}$ equal to 1% of A_f, frequency $f_{\text{sub-h}}$ variable in the range [5, 45] Hz with a frequency step equal to 0.25 Hz, and initial phase angle $\varphi_{\text{sub-h}}$ randomly (uniform distribution) variable in the range $[-\pi, \pi]$. The signals are numerically generated for a time duration of 10 s, and 100 initial phase angles $\varphi_{\text{sub-h}}$ are extracted for each subharmonic frequency. All the results reported in the following refer to the maximum errors obtained by using the random variation of the initial phase.

The simulation outputs are provided in Figs. 3 and 4 where the mean absolute values of ε_g and ε_{csg} evaluated over 10 s are reported along with their maximum values ξ_g and ξ_{csg}. As a general comment, it can be observed that signal processing has a slightly lower impact on the evaluation of Y_{csg} compared to Y_g, being the maximum ξ_g greater than the maximum ξ_{csg}. This is explained by considering that, in the evaluation of Y_{csg}, the tones at 5 and 45 Hz, introduced by the spectral leakage when the analyzed time frame is not an integer multiple of the signal

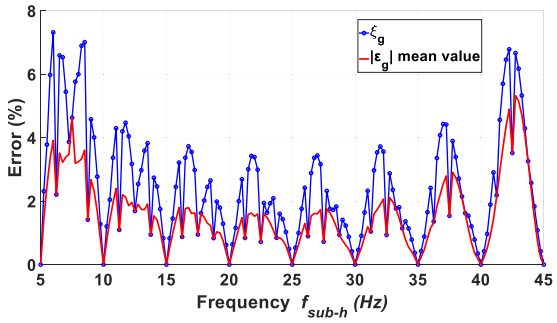

Fig. 3. Mean absolute value and maximum absolute value (ξ_g) of ε_g, introduced by the signal processing in the measurement of Y_g, versus the generated subharmonic frequency.

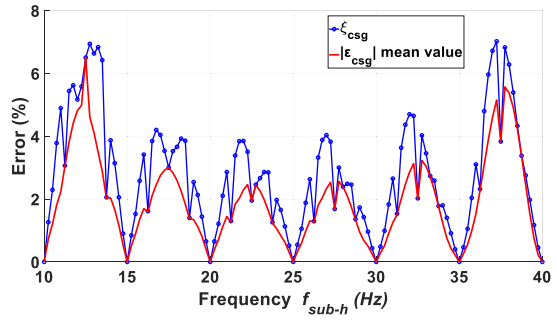

Fig. 4. Mean absolute value and maximum absolute value (ξ_{csg}) of ε_{csg}, introduced by the signal processing in the measurement of Y_{csg}, versus the generated subharmonic frequency.

period, are not included, and for this reason, the overall error is reduced. The maximum ξ_g is equal to 7.3%, and it is observed for $f_{\text{sub-h}}$ equal to 6 Hz, whereas the maximum ξ_{csg} is 6.9% at 12.75 Hz. It can be noticed that, for subharmonics with frequencies $f_{\text{sub-h}}$ integer multiple of 1.25 Hz, the ξ_η values are overlapped with the mean values of $|\varepsilon_\eta|$. In fact, when $s_1(t)$ [see (5)] is composed of a fundamental tone at 50 Hz and a subharmonic at a frequency integer multiple of 1.25 Hz, the period of $s_1(t)$ can be 800 (odd multiples of 1.25 Hz) or 400 ms (even multiples of 1.25 Hz). In this case, a time frame of 200 ms corresponds to a portion of the signal of, respectively, a quarter or a half of the period. The DFT, performed on nonoverlapped and consecutive portions of a quarter or a half of the period, produces the same magnitude spectra, implying that Y_η, and by extension ε_η, assumes a constant time behavior.

B. Case of Multiple Subharmonics

For this second case, the simulated signal is composed of a fundamental tone plus two subharmonics, as described in the following equation:

$$s_1(t) = A_f \sin(2\pi f_0 t) + A_{\text{sub-h}} \sin(2\pi f_{\text{sub-h}} t + \varphi_{\text{sub-h}}) + A_{\text{sub-h,out}} \sin\left(2\pi f_{\text{sub-h,out}} t + \varphi_{\text{sub-h,out}}\right). \quad (6)$$

The fundamental tone has amplitude A_f equal to 1 V and frequency f_0 fixed at 50 Hz; the first subharmonic has amplitude $A_{\text{sub-h}}$ equal to 1% of A_f, frequency $f_{\text{sub-h}}$ variable in the range [5, 45] Hz, and initial phase angle $\varphi_{\text{sub-h}}$ randomly (uniform distribution) variable in the range $[-\pi, \pi]$. The

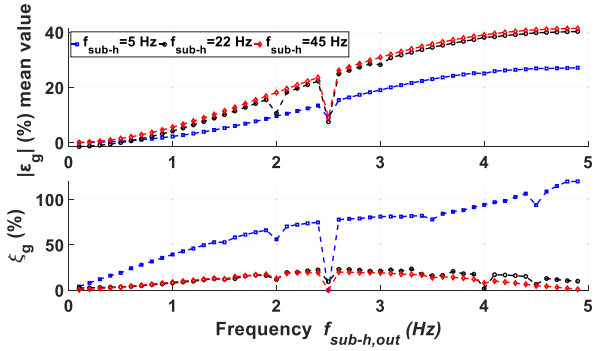

Fig. 5. Mean values of $|\varepsilon_g|$ and absolute maximum values ξ_g, introduced by the signal processing in the measurement of Y_g, when signals composed of tones with $f_{\text{sub-h}}$ equal to 5 (square marker), 22 (circle marker), and 45 Hz (diamond marker), and $f_{\text{sub-h,out}}$ in [0.1, 4.9] Hz range are analyzed.

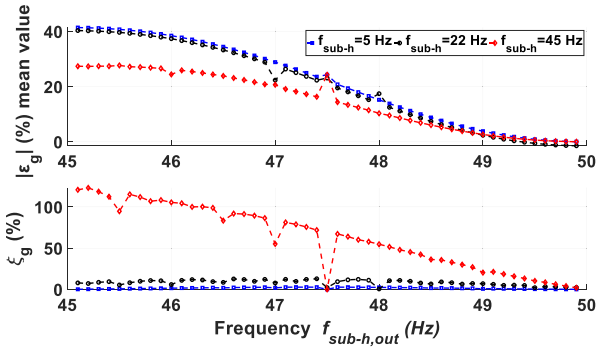

Fig. 6. Mean values of $|\varepsilon_g|$ and absolute maximum values ξ_g, introduced by the signal processing in the measurement of Y_g, when signals composed of tones with $f_{\text{sub-h}}$ equal to 5 (square marker), 22 (circle marker), and 45 Hz (diamond marker), and $f_{\text{sub-h,out}}$ in [0.1, 4.9] Hz range are analyzed.

second subharmonic has amplitude $A_{\text{sub-h,out}}$ equal to 1% of A_f, frequency $f_{\text{sub-h,out}}$ variable in the ranges [0.1, 4.9] and [45.1, 49.9] Hz, and initial phase angle $\varphi_{\text{sub-h,out}}$ randomly (uniform distribution) variable in the range $[-\pi, \pi]$. The signals are numerically generated for a time duration of 10 s, and 100 initial phase angles $\varphi_{\text{sub-h}}$ and $\varphi_{\text{sub-h,out}}$ are extracted for each subharmonic frequency. Also, in this case, all the reported results refer to the maximum errors obtained by using the random variation of the initial phase. For sake of brevity, only results related to ε_g at $f_{\text{sub-h}}$ equal to 5, 22, and 45 Hz are provided, but similar considerations also apply to ε_{csg} and different $f_{\text{sub-h}}$ frequencies.

As it can be observed in Figs. 5 and 6, even if $f_{\text{sub-h}}$ is an integer multiple of 5 Hz, the presence of subharmonic components outside the frequency range [5, 45] Hz leads ε_g to assume mean values and oscillations different from 0%. The worst cases are observed for the combinations with the lowest absolute value of the difference between $f_{\text{sub-h}}$ and $f_{\text{sub-h,out}}$, which are the combinations 5 Hz/4.9 Hz and 45 Hz/45.1 Hz. In these cases, oscillations up to 150% are found. On the contrary, the lowest variations are observed in the cases where $f_{\text{sub-h}}$ and $f_{\text{sub-h,out}}$ differ the most, i.e., the combinations 5 Hz/0.1 Hz, 45 Hz/0.1 Hz, and 5 Hz/49.9 Hz.

These results can be explained considering that the tones outside the range [5, 45] Hz produce leakage that distributes

TABLE I
SIMULATED ITS

ε (0.1 Hz) (%)	$\Delta\varphi$ (0.1 Hz) (rad)	ε (50 Hz) (%)	$\Delta\varphi$(50 Hz) (rad)
From -30 to 0	From -π/4 to 0	0	0

along the frequency spectrum, resulting in subharmonic components not present in the analyzed signal. As the distance between the frequencies $f_{\text{sub-h}}$ and $f_{\text{sub-h,out}}$ decreases, the leakages produced by the component at $f_{\text{sub-h,out}}$ and the tone at $f_{\text{sub-h}}$ combine in an additive way, resulting in higher errors.

IV. IMPACT OF INSTRUMENT TRANSFORMERS

This section analyses, through numerical simulations, how an IT coupled with a PQI affects the measurement of Y_g and Y_{csg}. In particular, the simulations have the main target of investigating the sensitivity of the IT error contributions, to the subharmonic measurements, with respect to the IT frequency response parameters. In other words, the simulations do not aim at accurately quantifying the error contribution of a specific type of IT to the measurement of subharmonics (performed according to [22]), but they are intended to show how the errors vary as the IT frequency responses change.

The in-force standards of the IEC 61869 family dealing with ITs do not indicate the performance requirements for the IT involved in the measurement of subharmonics. In this respect, the only information is provided in IEC 61869-6 [33], where the extension of the LPVT accuracy class for measurements at frequencies lower than the rated one is indicated. In particular, in [33], for each IT accuracy class, limits for the ratio and phase errors, defined according to (7) and (8), at 1 Hz are reported

$$\varepsilon(f_{\text{sub-h}}) = \frac{k_r \cdot V_s(f_{\text{sub-h}}) - V_p(f_{\text{sub-h}})}{V_p(f_{\text{sub-h}})} \tag{7}$$

$$\Delta\varphi(f_{\text{sub-h}}) = \sphericalangle \boldsymbol{V}_s(f_{\text{sub-h}}) - \sphericalangle \boldsymbol{V}_p(f_{\text{sub-h}}) \tag{8}$$

where

- $k_r = V_{p,r}/V_{s,r}$ — rated transformation ratio ($V_{p,r}$ and $V_{s,r}$ are the rated primary and secondary voltages);
- $V_p(f_{\text{sub-h}})$ and $V_s(f_{\text{sub-h}})$ — RMS values of the primary and secondary harmonic voltages at frequency $f_{\text{sub-h}}$;
- $\sphericalangle \boldsymbol{V}_p(f_{\text{sub-h}})$ and $\sphericalangle \boldsymbol{V}_s(f_{\text{sub-h}})$ — phase angles of the primary and secondary harmonic voltage phasors at $f_{\text{sub-h}}$.

Starting from this information, several scenarios are considered in the simulations, as reported in Table I. In all the cases, the IT ratio and phase errors at 50 Hz are set to zero, whereas the errors at 0.1 Hz change and go from the limits of [33] for a 0.5 accuracy class IT to zero. As a result, in the various cases, the IT frequency response has two fixed points at 0.1 and 50 Hz. For the union of these two points, infinite options would have been available, but any selection would have been unrepresentative of all the possible IT models. As a result, the simplest solution—a straight line connecting the points at 0.1 and 50 Hz—is chosen. While remaining completely general and not at all representative of any specific IT model, this option allows meeting the IEC 61869-6 [33] error limits. Some examples of the response of the simulated ITs at subharmonic frequencies are provided in Fig. 7.

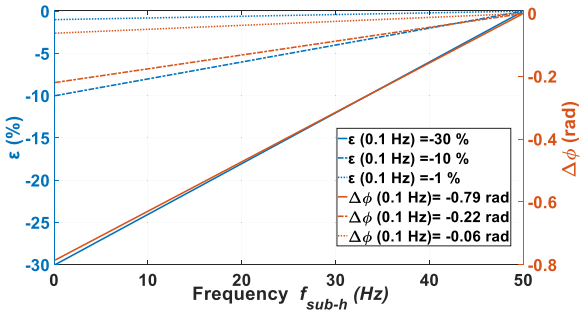

Fig. 7. Examples of simulated IT ratio and phase error responses at subharmonics frequencies.

It is worth noting that the numerical simulations described in this section have been run by considering all the possible combinations of the following:

1) IT frequency response according to Table I;
2) frequency and phase of the subharmonic inside the range [5, 45] Hz, according to (5);
3) frequency and phase of the subharmonic inside the ranges]0, 5[and]45, 50[Hz, according to (6).

However, since there are a number of variables in this analysis, for sake of clarity toward the reader, the results are presented in various steps, and in each step, some variables have a fixed value.

A. Case of a Single Subharmonic

In analogy to Section III-A, even with the presence of a simulated IT, the case of a single subharmonic is first analyzed. Here, all the possible combinations of: 1) IT frequency response according to Table I and 2) frequency and phase of the subharmonic inside the range [5, 45] Hz, according to (5), are considered. The IT error contributions are evaluated according to the IT-PI (4) introduced in Section II.

The main outcomes of this simulation are listed in the following and summarized in Table II.

As a first result, it is evidenced that, for $f_{\text{sub-h}}$ integer multiple of 5 Hz and for any combination of the IT ratio and phase error, the PI ε_g and ε_{csg} assume the same values of the IT ratio error at $f_{\text{sub-h}}$ with a constant time behavior.

For $\Delta\varphi$(0.1 Hz) equal to 0 rad and any value of ε(0.1 Hz), the indices ε_g and ε_{csg} do not oscillate over time, and they are overlapped with the IT ratio errors.

On the contrary, for $\Delta\varphi$(0.1 Hz) different from 0 rad, the indices ε_g and ε_{csg} assume mean values equal to the IT ratio errors but show an oscillating time behavior with a maximum absolute value up to seven times the IT ratio error.

For sake of clarity, Figs. 8 and 9 show, respectively, ξ_g and ξ_{csg} resulting from these simulations only in some specific conditions listed in the following.

1) ε(0.1 Hz) is fixed at -1%.

TABLE II

IMPACT OF ITS ON SUBHARMONICS MEASUREMENT: MAIN RESULTS OF THE SIMULATIONS WITH ONE SUBHARMONIC TONE

Simulation Parameters			Results
ε (0.1Hz)	$\Delta\varphi$(0.1 Hz)	$f_{\text{sub-h}}$	ε_g and ε_{csg}
Any value	Any value	Multiple of 5 Hz	Do not oscillate over time and assume values equal to ε ($f_{\text{sub-h}}$)
Any value	0	Any value	Do not oscillate over time and assume values equal to ε ($f_{\text{sub-h}}$)
Any value	Any value	Any value except for 5 Hz multiple	Oscillate over time and assume mean value equal to ε ($f_{\text{sub-h}}$)

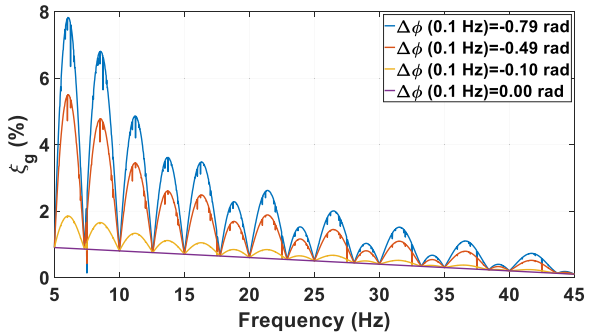

Fig. 8. Maximum error (ξ_g) introduced by linear ITs, with different phase error responses, in the measurement of Y_g versus the generated subharmonic frequencies.

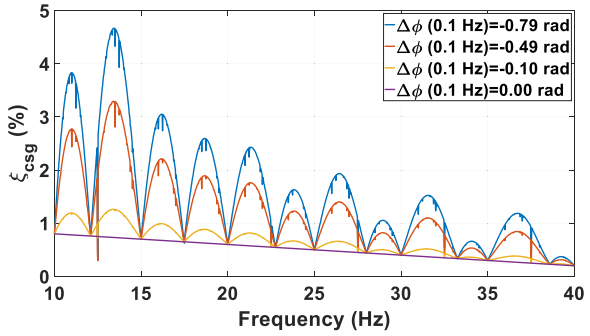

Fig. 9. Maximum error (ξ_{csg}) introduced by linear ITs, with different phase error responses, in the measurement of Y_{csg} versus the generated subharmonic frequencies.

2) Just four values of $\Delta\varphi$(0.1 Hz), the two cases that lead to the maximum and the minimum errors and two middle points, are shown.

In Figs. 8 and 9, looking to a particular value of $f_{\text{sub-h}}$ on the horizontal axis, an increase in the values of ξ_g and ξ_{csg} can be observed when Δ_φ(0.1 Hz) increases.

The maximum values of ξ_g and ξ_{csg} are 7.8% and 4.7%, and they are observed for $f_{\text{sub-h}}$ equal to 6 and 13 Hz, respectively, and for $\Delta\varphi$(0.1 Hz) equal to $-\pi/4$.

TABLE III

SIMULATED ITS USED IN THE CASE OF MULTIPLE SUBHARMONICS

Simulated ITs	ε (0.1 Hz) (%)	$\Delta\varphi$ (0.1 Hz) (rad)	ε (50 Hz) (%)	$\Delta\varphi$ (50 Hz) (rad)
IT_A	-1	-π/4	0	0
IT_B	-1	-0.20	0	0
IT_C	-1	-0.10	0	0

B. Case of Multiple Subharmonics

In analogy to Section III-B, the case of multiple subharmonics is then analyzed. Here, all the possible combinations of: 1) IT frequency response according to Table I; 2) frequency and phase of the subharmonic inside the range [5, 45] Hz, according to (5); and 3) frequency and phase of the subharmonic inside the ranges]0, 5[and]45, 50[Hz, according to (6), are been considered.

For sake of clarity, the results are presented in three steps.

In the first step, the analysis is carried out in the following conditions.

$$\xi_g = \xi_{\text{csg}} = \varepsilon_g = \varepsilon_{\text{csg}} = \varepsilon(15\text{ Hz}) \tag{9}$$

1) $f_{\text{sub-h}}$ is fixed to 15 Hz, that is, a tone included in both Y_g and Y_{csg}. The reason for this choice comes from the fact that, with the sole presence of this subharmonic, according to Figs. 8 and 9, at 15 Hz, the following condition applies:
2) This means that ε_g and ε_{csg} do not oscillate and are equal to ε(15 Hz). This, in turn, implies that it is possible to evaluate the oscillations introduced by the sole subharmonic outside the range [5, 45] Hz.
3) Three different ITs are considered and shown in Table III. In fact, since Section IV-A highlights that the IT phase error $\Delta_\varphi(f_{\text{sub-h}})$ represents the most critical element for the PIs, here, ε(0.1 Hz) is constant and equal to -1%. Δ_φ(0.1 Hz) has three different values that include the limit value for a phase error of [33].
4) The frequency and phase of the subharmonic inside the ranges]0, 5[and]45, 50[Hz, according to (6), are variable.

Due to the presence of such a subharmonic tone, the signals considered in this step have a periodicity that is not an integer submultiple of the 200-ms analyzed time frame. This fact leads ε_g and ε_{csg} to oscillate and have a mean value different from ε(15 Hz). In other words, (9) does not apply anymore.

Figs. 10 and 11 show, respectively, ξ_g and ξ_{csg} for the three simulated ITs (see Table III); they also show the absolute value of the IT ratio error $|\varepsilon(15\text{ Hz})| = 0.7\%$, equal for all the three simulated ITs.

As it can be observed, ξ_g and ξ_{csg} strongly depend on the phase errors of the simulated IT. When subharmonics in the [0.1, 4.9] Hz range are present [see Fig. 10(a) and 11(a)], the following maximum values of ξ_g and ξ_{csg} are found.

1) $\xi_g = 22.1\%$ and $\xi_{\text{csg}} = 14.3\%$ for IT_A.
2) $\xi_g = 6.3\%$ and $\xi_{\text{csg}} = 4.6\%$ for IT_B.
3) $\xi_g = 3.6\%$ and $\xi_{\text{csg}} = 2.7\%$ for IT_C.

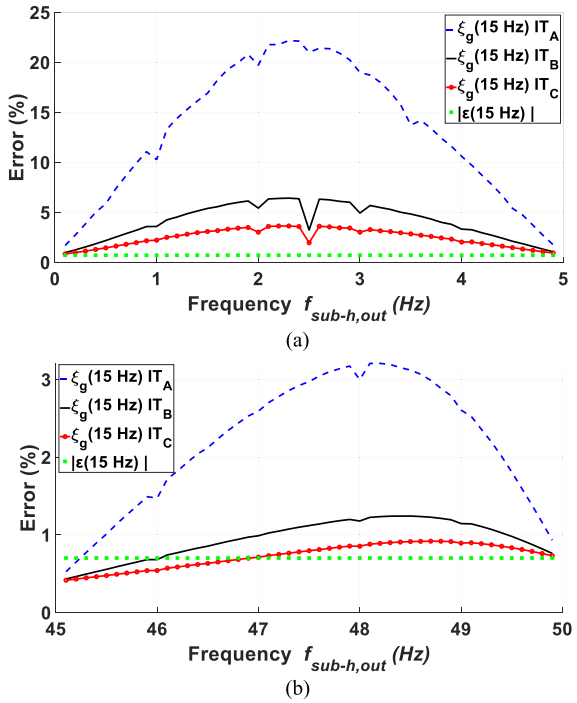

Fig. 10. Maximum error (ξ_g) introduced by linear ITs, with different phase error responses, when signals composed of tones with $f_{\text{sub-h}}$ equal to 15 Hz and $f_{\text{sub-h\_out}}$ in (a) [0.1, 4.9] Hz range and (b) [45.1, 49.9] Hz range are analyzed.

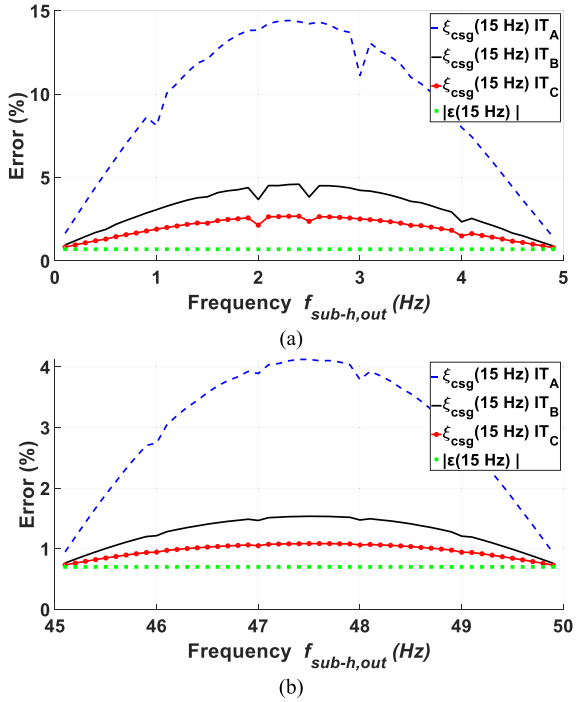

Fig. 11. Maximum error (ξ_{csg}) introduced by linear ITs, with different phase error responses, when signals composed of tones with $f_{\text{sub-h}}$ equal to 15 Hz and $f_{\text{sub-h\_out}}$ in (a) [0.1, 4.9] Hz range and (b) [45.1, 49.9] Hz range are analyzed.

It can be noticed that ξ_g and ξ_{csg} also strongly depend on the $f_{\text{sub-h,out}}$ values. By the comparison of Fig. 10(a) with Fig. 10(b), and Fig. 11(a) with Fig. 11(b), it can be observed that the maximum values of ξ_g and ξ_{csg} decrease between 70% and 80% when subharmonics in the [45.1, 49.9] Hz range are present instead of the subharmonics in the [0.1, 4.9] Hz range. In fact, for instance, looking at Fig. 10(a) and (b), for the IT$_A$, the maximum values of ξ_g are 21.8% and 3.2%, respectively. Looking at Fig. 11(a) and (b), for the IT$_A$, the maximum values of $\xi_{\text{csg}}$are 14.3% and 4.1%.

In general, we can observe the following.

1) For $f_{\text{sub-h,out}} < 5$ Hz [see Fig. 10(a) and 11(a)], both ξ_g and ξ_{csg} are greater than $|\varepsilon(15\text{ Hz})|$, and moreover, ξ_g is greater than ξ_{csg}.
2) Instead, for $f_{\text{sub-h,out}} > 45$ Hz, ξ_{csg} is always greater than $|\varepsilon(15\text{ Hz})|$ [see Fig. 11(b)], whereas ξ_g is lower than $|\varepsilon(15\text{ Hz})|$ for some frequencies [see Fig. 10(b)].

In order to understand these results, first, we have to consider that the errors of the simulated ITs in the range]0, 5[Hz are higher (in absolute value) than the errors in the range]45, 50[Hz. This condition, anyway, is generally valid for all the ITs for power system applications.

Therefore, with a $f_{\text{sub-h,out}} < 5$ Hz, the spectral leakages at the primary and secondary sides of the IT significantly differ among themselves, and this leads the errors ε_g and ε_{csg} to increase. Instead, with a $f_{\text{sub-h,out}} > 45$ Hz, the spectral leakages at the primary and secondary sides of the IT are very similar, and this leads the errors ε_g and ε_{csg} to decrease.

Moreover, since the components at $f_{\text{sub-h,out}} < 5$ Hz produce a more significant leakage in the first portion of the [5, 45] Hz range, ξ_{csg} is lower than ξ_g because Y_{csg} does not include the 5-Hz tone. Similarly, the components at $f_{\text{sub-h,out}} > 45$ Hz has a stronger influence on the last portion of [5, 45] Hz range and, for this reason, ξ_{csg} is higher than ξ_g.

In the second step, the analysis is carried out in the following conditions.

1) $f_{\text{sub-h,out}}$ is fixed to 4.9 Hz. In fact, from the analysis of the results of all the numerical simulations, the worst case resulted in the combination of two subharmonics: one with $f_{\text{sub-h}} = 6$ Hz and one with $f_{\text{sub-h,out}} = 4.9$ Hz. For sake of clarity, this particular condition is not presented before, but it is considered in the following.
2) An IT having $\Delta\varphi(0.1\text{ Hz}) = -\pi/4$ rad and $\varepsilon(0.1\text{ Hz}) = -30\%$ (-30% and $-\pi/4$ rad are the limits of [33] for a class 0.5 IT) is considered. As in the previous point, this case produced the worst results. Again, for sake of clarity, this particular condition is not presented before, but it is considered in the following.
3) The frequency and phase of the subharmonic inside the range [5, 45] Hz are variable.

Fig. 12 shows the behavior of ξ_g and the mean value of $|\varepsilon_g|$ when $f_{\text{sub-h}}$ varies. The behavior of ξ_{csg} and the mean value of $|\varepsilon_{\text{csg}}|$ are not shown since they are lower than, respectively, ξ_g and the mean value of $|\varepsilon_g|$.

As it can be observed, the maximum value of ξ_g is equal to 54.5%, and it is found when $f_{\text{sub-h}}$ is equal to 6 Hz.

In the third step, the analysis is carried out in the following conditions.

1) $f_{\text{sub-h}}$ and $f_{\text{sub-h,out}}$ are fixed to, respectively, 6 and 4.9 Hz. This choice is made since, from the results of

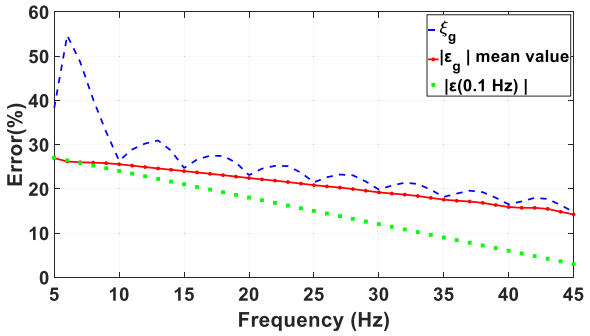

Fig. 12. ξ_g (dotted line), mean value of the maximum absolute value of ε_g (circle marker), and mean value of the absolute value of $\varepsilon(0.1\text{ Hz})$ (square marker) measured when the signal has a tone at $f_{\text{sub-h,out}} = 4.9$ Hz and another one at $f_{\text{sub-h}}$ in the [5, 45] Hz range.

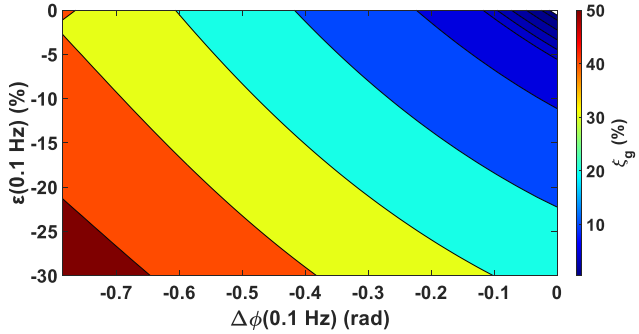

Fig. 13. Maximum value of ξ_g versus IT ratio and phase errors at 0.1 Hz.

the first and second steps, this particular combination gives the worst error condition.

2) $\varepsilon(0.1\text{ Hz})$ and $\Delta\varphi(0.1\text{ Hz})$ are variables in the ranges shown in Table I.

Fig. 13 shows the behavior of ξ_g versus $\varepsilon(0.1\text{ Hz})$ and $\Delta\varphi(0.1\text{ Hz})$. We can observe the following.

1) The maximum value of ξ_g is 54.5%, obtained for $\varepsilon(0.1\text{ Hz}) = -30\%$ and $\Delta\varphi(0.1\text{ Hz}) = -\pi/4$ rad.
2) ξ_g is equal to 0% when $\varepsilon(0.1\text{ Hz}) = 0\%$ and $\Delta\varphi(0.1\text{ Hz}) = 0$ rad.
3) ξ_g is lower than 10% when $|\varepsilon(0.1\text{ Hz})| < 9.5\%$ and $\left|\Delta_\varphi(0.1\text{ Hz})\right| < 62$ mrad.
4) ξ_g is lower than 3% when $|\varepsilon(0.1\text{ Hz})| < 2\%$ and $\left|\Delta_\varphi(0.1\text{ Hz})\right| < 30$ mrad.

C. Comments on the Results of the Numerical Analysis

Sections IV-A and IV-B have analyzed, through numerical simulations, the impact on the measurement of subharmonics in the range [5, 45] Hz, in compliance with [22], of the frequency response parameters of linear ITs, compliant with the IEC 61869 standard family. The main outcomes of the simulations are summarized in the following.

1) When the IT phase error is different from zero in the [0.1, 49.9] Hz frequency range, it introduces time-varying errors ε_g and ε_{csg}.
2) The maximum absolute values of ε_g and ε_{csg}(ξ_g and ξ_{csg}) strongly depend on the IT phase error responses, whereas their mean values depend on the IT ratio errors.

TABLE IV
RATED CHARACTERISTICS OF THE ANALYZED VTS

Type	Accuracy Class	Rated Primary Voltage (kV)	Rated Secondary Voltage (V)	Rated Burden (VA)
LPVT	1	10	100	5
Inductive VT	0.5	3	100	25

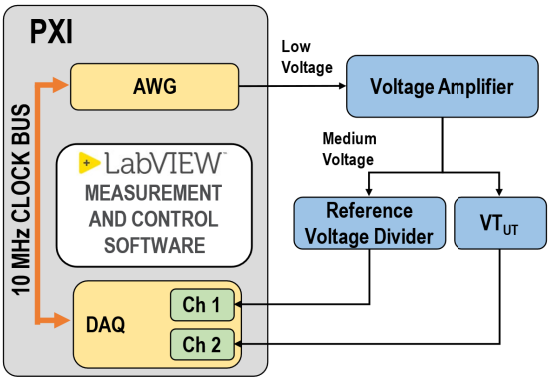

Fig. 14. Block diagram of the generation and measurement setup for the MV VT under test.

3) The amplitude of ξ_g and ξ_{csg} can dramatically increase when the IT is supplied also with subharmonics in the [0.1, 4.9] Hz frequency range. In this case, the observed ξ_g are always greater than ξ_{csg}, and the maximum errors are found for the combination of the tones at $f_{\text{sub-h}}$ equal to 6 Hz and $f_{\text{sub-h,out}}$ equal to 4.9 Hz.
4) On the contrary, the presence of subharmonics in the [45.1, 49.9] Hz range in the IT input signal has a lower impact on ε_g and ε_{csg} compared to the case of subharmonics in the [0.1, 4.9] Hz range.

V. MEASUREMENT SETUP

Several commercial VTs were tested in order to quantify the impact of VTs on the measurement of subharmonics and give experimental evidence of the main results shown in Section IV. However, for sake of brevity, in the following, only the results related to two commercial VTs (one inductive VT and one LPVT based on capacitive sensing technology) for MV phase to ground measurement applications are shown.

The VTs' main features are summarized in Table IV. The generation and measurement setup are shown in Fig. 14. The reference voltage signal to be applied to the VTs under test is provided by an Arbitrary Waveform Generator (AWG) National Instrument (NI) PCI eXtension for Instrumentation (PXI) 5422 (16 bit, variable output gain, ±12-V output range, 200-MHz maximum sampling rate, and 256-MB onboard memory). The AWG generates a 4-MHz clock that is used to derive the sampling clock; this allows obtaining coherent sampling, thus avoiding spectral leakage. Acquisition of the primary and secondary waveforms of the VT under test has been performed through the data acquisition board PXIe-6124 (±10 V, 16 bit, and maximum sampling rate: 4 MHz).

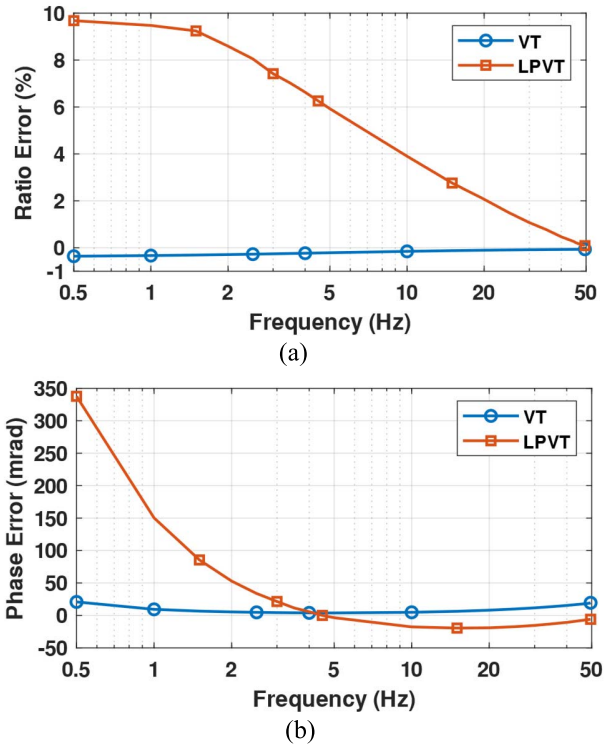

Fig. 15. (a) Ratio errors and (b) phase errors of the inductive VT (circle marker) and the LPVT (square marker) under test.

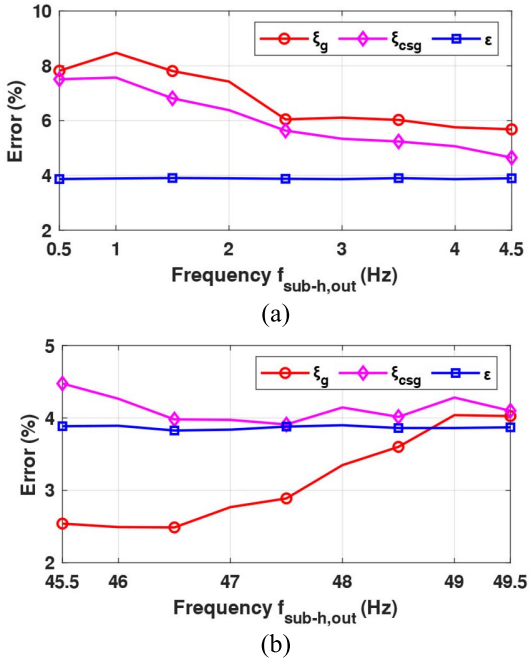

Fig. 16. LPVT: the maximum absolute value of the interharmonic group (ξ_g), the maximum absolute value of the centered interharmonic subgroup (ξ_{csg}), and the ratio error at the second subharmonic frequency (ε at 10 Hz) from (a) 0.5 to 4.5 Hz and (b) 45.5 to 49.5 Hz.

Waveforms have been sampled with a 10-kHz rate obtained through oversampling in order to reduce the impact of noise. The output of the AWG is connected to an HV power amplifier (NF HVA4321, up to 10 kV, from 0 Hz up to 30 kHz) feeding the VT under test. Primary voltages are scaled by an Ohm-Labs KV-10A HV divider (HVD) with a ratio of 1000 V/V. The ratio and phase error of the HVD from 0 up to 50 Hz are below 105 μV/V and 120 μrad with an extended uncertainty (level of confidence 95%) of 50 μV/V and 50 μrad. The uncertainty of ratio error includes the amplitude nonlinearity contribution equal to 30 μV/V.

VI. Experimental Results

This section discusses the experimental tests performed on the two considered VTs. The same test signals used in Sections III and IV are generated through the measurement setup presented in Section V.

A. Characterization of VTs at Subharmonic Frequencies

In Fig. 15, the ratio [see Fig. 15(a)] and phase [see Fig. 15(b)] errors are shown for the LPVT and the inductive VT under test.

In this characterization, the test waveform is composed of the fundamental tone at 50 Hz and the rated amplitude with a single superimposed subharmonic with a fixed amplitude of 3% and a frequency variable in the range [0.5, 49.5] Hz. This is called the FS test (fundamental plus one subharmonic). The evaluation of ratio and phase errors is performed over an integer number of periods of the FS signal in nonoverlapped time frames [34]. This test aims at providing the low-frequency characterization of the transformer under test; in fact, the obtained ratio and phase errors can be assumed as the reference performance of the VTs under test when they are used to measure voltage subharmonics in the frequency range [0.5, 49.5] Hz. In these tests, the following conditions apply: 1) there is only one subharmonic tone and 2) the spectral analysis is performed over a time frame that represents an integer number of the signal period. This implies that the amplitude of the single subharmonic tone is practically coincident with Y_g and Y_{csg}, and so ε, ε_g, and ε_{csg} have the same value. As it can be seen, the ratio and phase errors of the inductive VT under test range from -0.4% at 0.5 Hz up to 0.1% at 49.5 Hz and from 20 mrad at 0.5 Hz up to 4 mrad at 4 Hz, respectively, so having a quite flat behavior, compared to its accuracy class error limits. The ratio and phase errors of the LPVT under test range from 9.7% at 0.5Hz up to 0.1% at 49.5Hz and from 338 mrad at 0.5 Hz up to -19.5 mrad at 15 Hz, respectively, so having a worse behavior, with respect to its accuracy class error limits.

B. Performance of the VTs Under Test in Presence of Two Subharmonics

Figs. 16 and 17 show ξ_g and ξ_{csg} in different test conditions. The test waveform is composed of the fundamental tone at 50 Hz and rated amplitude, and two superimposed subharmonic tones. The first subharmonic is fixed at 10 Hz and has an amplitude equal to 3% of the fundamental tone. The second subharmonic has the same amplitude (3%) and frequency variable in the ranges [0.5, 4.5] and [45.5, 49.5] Hz.

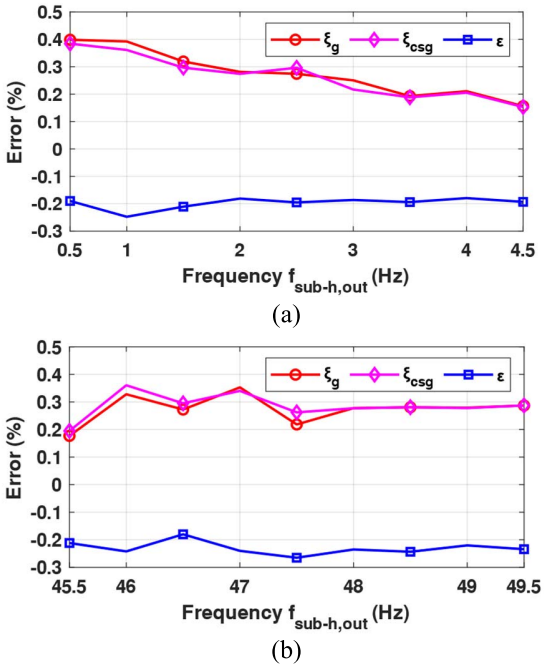

Fig. 17. Inductive VT: the maximum absolute value of the interharmonic group (ξ_g), the maximum absolute value of the centered interharmonic subgroup (ξ_{csg}), and the ratio error at the second subharmonic frequency (ε at 10 Hz) from (a) 0.5 to 4.5 Hz and (b) 45.5 to 49.5 Hz.

Figs. 16 and 17 also report the ratio error $\varepsilon(10\ \text{Hz})$ of the VTs, evaluated by considering a time frame equal to an integer number of periods of the signal (so considering also the periodicity of the fundamental and of the additional subharmonic tone).

Figs. 16(a) and (b) show ξ_g and ξ_{csg} for the LPVT when the second subharmonic tone frequency $f_{sub-h,out}$ varies, respectively, in the ranges [0.5, 4.5] and [45.5, 49.5] Hz. As it can be seen, there is a remarkable difference between $\varepsilon(10\ \text{Hz})$ and the indexes ξ_g and ξ_{csg}. In fact, it results in that $\varepsilon(10\ \text{Hz}) = 4\%$ [in Fig. 16(a) and (b)], whereas the following holds.

1) ξ_g ranges from 8.5% when $f_{sub-h,out} = 1$ Hz down to 5.7% when $f_{sub-h,out} = 4.5$ Hz [see Fig. 16(a)].
2) ξ_g ranges from 2.5% when $f_{sub-h,out} = 46.5$ Hz up to 4% when $f_{sub-h,out} = 49.5$ Hz [see Fig. 16(b)].
3) ξ_{csg} ranges from 7.5% when $f_{sub-h,out} = 0.5$ Hz down to 4.6% when $f_{sub-h,out} = 4.5$ Hz [see Fig. 16(a)].
4) ξ_{csg} ranges from 4.5% when $f_{sub-h,out} = 45.5$ Hz down to 3.9% when $f_{sub-h,out} = 47.5$ Hz [see Fig. 16(b)].

It is worth noting that ξ_g and ξ_{csg} behave differently in the two different frequency ranges, in accordance to the simulation results discussed in Section IV.

Fig. 17(a) and (b) shows the measured ξ_g and ξ_{csg} for the inductive VT when the second subharmonic tone frequency $f_{sub-h,out}$ varies, respectively, in the ranges [0.5, 4.5] and [45.5, 49.5] Hz. Also here, there is a difference between $\varepsilon(10\ \text{Hz})$ and the indexes ξ_g and ξ_{csg}. In fact, it results in that $\varepsilon(10\ \text{Hz})$ is about -0.2% [in Fig. 17(a) and (b)], whereas the following holds.

1) ξ_g ranges from 0.4% when $f_{sub-h,out} = 0.5$ Hz down to 0.15% when $f_{sub-h,out} = 4.5$ Hz [see Fig. 17(a)].
2) ξ_g ranges from 0.2% when $f_{sub-h,out} = 45.5$ Hz up to 0.3% when $f_{sub-h,out} = 49.5$ Hz [see Fig. 17(b)].
3) ξ_{csg} ranges from 0.38% when $f_{sub-h,out} = 0.5$ Hz down to 0.14% when $f_{sub-h,out} = 4.5$ Hz [see Fig. 17(a)].
4) ξ_{csg} ranges from 0.22% when $f_{sub-h,out} = 45.5$ Hz down to 0.35% when $f_{sub-h,out} = 46.5$ Hz [see Fig. 17(b)].

For the inductive VT under test, which has a quite flat ratio and phase errors (compared to the limits of its accuracy class), as shown in Fig. 15(a) and (b), the difference between ξ_g and ξ_{csg} is negligible.

As a general comment on the experimental results, they mainly show that there are cases in which the errors introduced by a VT in the measurement of the first interharmonic group (ξ_g or ξ_{csg}) are equal to twice the errors of the same VT obtained through the laboratory characterization procedure (ratio error ε). This result is observed for all the tested VTs, even if here only two VTs are presented for sake of brevity and clarity. It is worthwhile noting that this result is here observed for two VTs based on different operating principles and different low-frequency responses. In fact, for the LPVT, $|\varepsilon(10\ \text{Hz})|$ is equal to 4%, whereas ξ_g reaches 8.5%. In the same test conditions, the inductive VT has $|\varepsilon(10\ \text{Hz})|$ equal to 0.2%, whereas ξ_g reaches 0.4%.

These results imply that, with the signal processing suggested by [22], it is not possible to compensate for VT errors by using the frequency response data measured during laboratory characterization. Instead, the use of different DFT windows [30] or measurement techniques [31], [32] that reduce or avoid spectral leakage would ensure that the maximum VT error ξ_g coincides with the ratio error $|\varepsilon|$. As a result, in these cases, more accurate measurements of the power system subharmonics could be obtained by correcting for the VT ratio error at subharmonics frequency, which would represent a systematic error.

VII. Conclusion

This article has analyzed from a numerical and an experimental point of view the performance of VTs when used to measure subharmonics in compliance with the international standards IEC 61869 family and IEC 61000-4-7.

The main outcomes of the work can be summarized as follows.

1) For the evaluation of the performance of the IT at subharmonic frequencies, extensions (ε_g and ε_{csg}) of the definition of the ratio error (ε), including the interharmonic group (Y_g) and the centered interharmonic subgroup (Y_{csg}), have been proposed.
2) According to IEC 61000-4-7 suggestions and considering the case of power frequency constant and equal to 50 Hz, Y_g and Y_{csg}, and consequently also ε_g and ε_{csg}, must be evaluated over time frames of 200 ms. This causes ε_g and ε_{csg} to have a not constant time behavior when subharmonics having a period not equal to an integer submultiple of 200 ms are present in the signal.

3) For this reason, the maximum absolute values of ε_g and ε_{csg} are always higher than the ratio error of the IT (supposing to evaluate the ratio error over a time frame integer multiple of the signal period). In presence of subharmonics in the range [5, 45] Hz ([10, 40] Hz), the value of ε_g (ε_{csg}) averaged over time is equal to the ratio error.
4) In the presence also of subharmonics outside the range [5, 45] Hz, ε_g and ε_{csg} strongly increase, and their value, even averaged over time, is higher than the ratio error of the IT.
5) Experimental test of commercial VTs (inductive and low power) has shown that ε_g and $\varepsilon_{\mathrm{csg}}$ can double the value of the ratio error at subharmonic frequencies.

Particularly, this last point induces a concluding remark. The performance of a VT at subharmonic frequencies is generally worse than that at power frequency. Therefore, for accurate subharmonic measurements according to IEC 61000-4-7, particular attention should be paid to the choice of the accuracy class to avoid an excessive loss of accuracy at low frequencies.

REFERENCES

[1] S. Bhattacharyya and S. Cobben, "Consequences of poor power quality—An overview," in *Power Quality*, A. Eberhard, Ed. InTech, 2011. [Online]. Available: http://www.intechopen.com/books/power-quality/consequences-of-poor-power-quality-an-overview

[2] S. Elphick, V. Gosbell, V. Smith, S. Perera, P. Ciufo, and G. Drury, "Methods for harmonic analysis and reporting in future grid applications," *IEEE Trans. Power Del.*, vol. 32, no. 2, pp. 989–995, Apr. 2017.

[3] L. Peretto, "The role of measurements in the smart grid era," *IEEE Instrum. Meas. Mag.*, vol. 13, no. 3, pp. 22–25, Jun. 2010.

[4] *Voltage Characteristics of Electricity Supplied by Public Distribution Networks*, Standard IEC EN 50160, May 2011.

[5] *Electromagnetic Compatibility (EMC)—Part 3-40: Testing and Measurement techniques—Power Quality Measurement Methods*, Standard IEC 61000-4-30, 2015.

[6] *Assessment of Power Quality—Characteristics of Electricity Supplied by Public Networks*, Standard IEC 62749, Feb. 2020.

[7] *Power Quality Measurement in Power Supply Systems—Part 1: Power Quality Instruments (PQI)*, Standard IEC 62586-1, 2014.

[8] *Power Quality Measurement in Power Supply Systems—Part 2: Functional Tests and Uncertainty Requirements*, Standard IEC 62586-2, 2014.

[9] *IEEE Recommended Practice for Monitoring Electric Power Quality*, IEEE Standard 1159, 2019.

[10] M. Kaczmarek and S. Jama, "Accuracy of inductive voltage transformer in the presence of voltage high harmonics," in *Proc. ICHVE Int. Conf. High Voltage Eng. Appl.*, Sep. 2014, pp. 1–4, doi: 10.1109/ICHVE.2014.7035462.

[11] S. Toscani, M. Faifer, A. Ferrero, C. Laurano, R. Ottoboni, and M. Zanoni, "Compensating nonlinearities in voltage transformers for enhanced harmonic measurements: The simplified Volterra approach," *IEEE Trans. Power Del.*, vol. 36, no. 1, pp. 362–370, Feb. 2021.

[12] G. Crotti *et al.*, "Instrument transformers for power quality measurements: A review of literature and standards," in *Proc. IEEE 11th Int. Workshop Appl. Meas. Power Syst. (AMPS)*, Oct. 2021, pp. 1–6.

[13] T. Pfajfar, J. Meyer, P. Schegner, and I. Papič, "Influence of instrument transformers on harmonic distortion assessment," in *Proc. IEEE Power Energy Soc. Gen. Meeting*, Jul. 2012, pp. 1–6, doi: 10.1109/PESGM.2012.6345309.

[14] *Instrument Transformers—Part 103: The Use of Instrument Transformers for Power Quality Measurement*, Standard IEC 61869-103, 2012.

[15] M. Wu, L. Xie, L. Cheng, and R. Sun, "A study on the impact of wind farm spatial distribution on power system sub-synchronous oscillations," *IEEE Trans. Power Syst.*, vol. 31, no. 3, pp. 2154–2162, May 2016.

[16] Z. Leonowicz, "Power quality in wind power systems," *Renew. Energy Power Qual. J.*, vol. 1, no. 7, pp. 234–238, Apr. 2009.

[17] G. Chen, C. Liu, G. Wang, D. Ai, H. Shi, and Y. Li, "Research on simulation accuracy of ultra-low frequency oscillation in power system with high proportion of hydropower," in *Proc. IEEE 3rd Int. Electr. Energy Conf. (CIEEC)*, Sep. 2019, pp. 834–838.

[18] R. Langella, A. Testa, S. Z. Djokic, J. Meyer, and E. M. Klatt, "On the interharmonic emission of PV inverters under different operating conditions," in *Proc. 17th Int. Conf. Harmon. Quality Power (ICHQP)*, Oct. 2016, pp. 733–738.

[19] R. F. Chu and J. J. Burns, "Impact of cycloconverter harmonics," *IEEE Trans. Ind. Appl.*, vol. 25, no. 3, pp. 427–435, May 1989.

[20] P. Syam, P. K. Nandi, and A. K. Chattopadhyay, "An improved feedback technique to suppress subharmonics in a naturally commutated cycloconverter," *IEEE Trans. Ind. Electron.*, vol. 45, no. 6, pp. 950–953, Dec. 1998.

[21] G. Crotti, G. D'Avanzo, P. Sara Letizia, and M. Luiso, "Measuring harmonics with inductive voltage transformers in presence of subharmonics," *IEEE Trans. Instrum. Meas.*, vol. 70, 2021, Art. no. 9005013.

[22] *Electromagnetic Compatibility (EMC)—Part 4-7: Testing and Measurement Techniques—General Guide on Harmonics and Interharmonics Measurements and Instrumentation, for Power Supply Systems and Equipment Connected Thereto*, Standard IEC 61000-4-7, 2008.

[23] *IEEE Recommended Practice for Monitoring Electric Power Quality*, IEEE Standard 1159, 2019.

[24] C. Li, W. Xu, and T. Tayjasanant, "Interharmonics: Basic concepts and techniques for their detection and measurement," *Electr. Power Syst. Res.*, vol. 66, no. 1, pp. 39–48, 2003, doi: 10.1016/S0378-7796(03)00070-1.

[25] G. Crotti *et al.*, "Measurement methods and procedures for assessing accuracy of instrument transformers for power quality measurements," in *Proc. Conf. Precis. Electromagn. Meas. (CPEM)*, Aug. 2020, pp. 1–2, doi: 10.1109/CPEM49742.2020.9191698.

[26] *Instrument Transformers—Part 2: Additional Requirements for Current Transformers*, Standard IEC 61869-2, 2012.

[27] *Instrument Transformers—Part 3: Additional Requirements for Inductive Voltage Transformers*, Standard IEC 61869-3, 2011.

[28] A. Arranz-Gimon, A. Zorita-Lamadrid, D. Morinigo-Sotelo, and O. Duque-Perez, "Analysis of the use of the Hanning Window for the measurement of interharmonic distortion caused by close tones in IEC standard framework," *Electr. Power Syst. Res.*, vol. 206, May 2022, Art. no. 107833, doi: 10.1016/j.epsr.2022.107833.

[29] T. Tarasiuk, "Comparative study of various methods of DFT calculation in the wake of IEC Standard 61000-4-7," *IEEE Trans. Instrum. Meas.*, vol. 58, no. 10, pp. 3666–3677, Oct. 2009, doi: 10.1109/TIM.2009.2019308.

[30] A. Testa, D. Gallo, and R. Langella, "On the processing of harmonics and interharmonics: Using Hanning window in standard framework," *IEEE Trans. Power Del.*, vol. 19, no. 1, pp. 28–34, Jan. 2004, doi: 10.1109/TPWRD.2003.820437.

[31] I. Y.-H. Gu and M. H. J. Bollen, "Estimating interharmonics by using sliding-window ESPRIT," *IEEE Trans. Power Del.*, vol. 23, no. 1, pp. 13–23, Jan. 2008, doi: 10.1109/TPWRD.2007.911130.

[32] A. Bracale, G. Carpinelli, Z. Leonowicz, T. Lobos, and J. Rezmer, "Measurement of IEC groups and subgroups using advanced spectrum estimation methods," *IEEE Trans. Instrum. Meas.*, vol. 57, no. 4, pp. 672–681, Apr. 2008, doi: 10.1109/TIM.2007.911701.

[33] *Instrument Transformers—Part 6: Additional General Requirements for Low-Power Instrument Transformers*, Standard IEC 61869-6, 2016.

[34] G. Artale *et al.*, "Measurement of simplified Single- and three-phase parameters for harmonic emission assessment based on IEEE 1459–2010," *IEEE Trans. Instrum. Meas.*, vol. 70, 2021, Art. no. 9000910, doi: 10.1109/TIM.2020.3037949.

Gabriella Crotti graduated *cum laude* in physics from the University of Turin, Turin, Italy, in 1986.

Since then, she has been with the Istituto Nazionale di Ricerca Metrologica (INRIM), Turin, where she currently works as a Director Technologist at the Electric and Electromagnetic Field and System Sector. She is leading the EMPIR project 19NRM05 IT4PQ. Her research interests are focused on the development and characterization of references and techniques for voltage and current measurements in high- and medium-voltage grids and on the traceability of electric and magnetic field measurements at low and intermediate frequencies.

Giovanni D'Avanzo was born in Naples, Italy, in 1991. He received the M.Sc. degree (*summa cum laude*) in electronic engineering from the University of Campania "Luigi Vanvitelli," Aversa, Italy, where he is currently pursuing the Ph.D. degree in energy conversion.

He is currently with Ricerca sul Sistema Energetico S.p.A., Milan, Italy. He is working on various European metrology research projects. His research interests include the characterization of instrument transformers under power quality phenomena, the development of smart meters, and measurement systems for e-vehicles.

Palma Sara Letizia was born in Caserta, Italy, in 1992. She received the M.Sc. degree (*summa cum laude*) in power electronic engineering from the University of Campania "Luigi Vanvitelli," Aversa, Italy. She is currently pursuing the Ph.D. degree in metrology with the Politecnico di Torino, Turin, Italy, and the Istituto Nazionale di Ricerca Metrologica (INRIM), Turin.

Her main scientific interest is metrology applied to power grids, in particular, the development of new procedures and reference sensors for power quality and phasor measurement unit applications and the definition of traceable characterization methods for medium-voltage transducers under nonsinusoidal conditions.

Mario Luiso (Member, IEEE) was born in Naples, Italy, in July 1981. He received the Laurea degree (*summa cum laude*) in electronic engineering and the Ph.D. degree in electrical energy conversion from the University of Campania "Luigi Vanvitelli," Aversa, Italy, in 2005 and 2007, respectively.

He is currently an Associate Professor with the Department of Engineering, University of Campania "Luigi Vanvitelli." He is the author or a coauthor of more than 200 papers published in books, scientific journals, and conference proceedings. His main scientific interests are related to the development of innovative methods, sensors, and instrumentation for power system measurements, in particular, power quality, calibration of instrument transformers, phasor measurement units, and smart meters.

Dr. Luiso is a member of the IEEE Instrumentation and Measurement Society.